

Imaging of lateral spin valves with soft X-ray microscopy

O. Mosendz,* G. Mihajlović, and J. E. Pearson

Materials Science Division, Argonne National Laboratory, Argonne, Illinois 60439, USA

P. Fischer and M.-Y. Im

Center for X-ray Optics, Lawrence Berkeley National Laboratory, Berkeley, California 94720, USA

S. D. Bader and A. Hoffmann†

*Materials Science Division and Center for Nanoscale Materials,
Argonne National Laboratory, Argonne, Illinois 60439, USA*

(Dated: November 17, 2018)

We investigated Co/Cu lateral spin valves by means of high-resolution transmission soft x-ray microscopy with magnetic contrast that utilizes x-ray magnetic circular dichroism (XMCD). No magnetic XMCD contrast was observed at the Cu L_3 absorption edge, which should directly image the spin accumulation in Cu. Although electrical transport measurements in a non-local geometry clearly detected the spin accumulation in Cu, which remained unchanged during illumination with circular polarized x-rays at the Co and Cu L_3 absorption edges.

PACS numbers: 72.25.Hg, 73.40.Jn, 75.25.+z, 75.75.+a

I. INTRODUCTION

Recent developments in spintronics showed that the use of spin polarized currents can have a profound impact on applications such as magnetic information processing and storage. Furthermore, the study of pure spin currents instead of spin polarized charge currents is providing a promising new direction to advance the present technology.^{1,2} Pure spin currents can be generated via a spin polarized charge current injection from ferromagnets,³ spin Hall effects,⁴ or spin pumping.^{5,6,7} In order to utilize pure spin currents it is necessary to understand their propagation properties. To this end, the direct imaging of a non-equilibrium spin accumulation that accompanies pure spin currents can generate new insights into the dynamic behavior of spins. This became evident from prior research on semiconducting systems, where such imaging is made possible due to strong magneto-optic effects.^{8,9,10,11,12} From such magneto-optical measurements it was discovered in semiconductors that spin coherence times are relatively long and injected spins can be transported with charge currents over macroscopic distances;⁸ spin Hall effects are detectable;^{9,10} the imaging revealed the flow-pattern of electrically injected spins including a spin back-diffusion against the charge current at the draining contact;¹¹ and spin polarization can be generated via spin-dependent reflection from metal-semiconductor interfaces.¹²

For metallic spin transport systems such direct imaging of the spin accumulation and spin currents remains elusive. One reason is that due to the smaller spin diffusion lengths, which are typically far in the submicron range,¹³ standard optical techniques do not provide sufficient spatial resolution. Nevertheless, it can be expected that successful imaging of the spin accumulation in metals will greatly enhance our understanding of spin currents and dynamics. Some questions that could be immediately

addressed are how spin currents couple to charge drift currents in metals¹⁴ and what role inhomogeneous spin injection plays for contacts whose sizes are comparable to the spin diffusion length.¹⁵

Soft x-ray microscopy with state-of-the-art Fresnel zone plates used as high resolution optics¹⁶ is a promising approach towards the goal of imaging spin accumulations in metals. The spatial resolution, down to 10 nm, is sufficiently high and it is possible to get magnetic contrast via x-ray magnetic circular dichroism (XMCD).^{17,18} Here we show investigations of Co/Cu lateral spin valves, which were imaged using magnetic transmission soft x-ray microscopy (MTXM) with circular polarized x-rays for detecting XMCD from the spin accumulation in Cu. Although the presence of a spin accumulation was verified with non-local transport measurements, there was no detectable XMCD contrast at the Cu L_3 absorption edge.

II. EXPERIMENTAL

The Co/Cu lateral spin valves were fabricated by means of e-beam lithography utilizing a double-layer PMMA/PMGI resist on a SiN/Si substrate. Selectively removing the Si enabled the SiN layer to be used as a free-standing x-ray transparent membrane, which is required to perform the MTXM imaging experiment. In order to minimize detrimental absorption we used a 100-nm thick SiN layer. Ohmic junctions for the lateral spin valves were formed by employing a lithographically controlled e-beam resist undercut technique with subsequent shadow mask evaporation of 25-nm Co and 80-nm Cu.¹⁹ After their fabrication, the lateral spin valves were covered by a 100 nm thick SiN protective layer deposited via *rf*-sputtering. Finally, the membrane windows were defined with photolithography on the substrate back-side

and the Si was removed via wet etching in a 30 % KOH solution. This process resulted in Co/Cu lateral spin valves sandwiched on both sides by 100 nm thick SiN layers forming a free-standing membrane.

All MTXM imaging was performed at beamline 6.1.2 (XM-1) of the Advanced Light Source. This microscope achieves 15 nm spatial resolution using state-of-the-art Fresnel zone plates and enables magnetic contrast via XMCD.^{17,18} During the measurements the synchrotron operated in a multibunch, top-off mode delivering a continuous electron beam-current of 400 mA. The beam position stability and the constant beam current in the top-off mode was beneficial for the long-term stability of the experiment, which accumulated x-ray images for two consecutive days. For the MTXM imaging we chose incident energies of 777 eV and 932 eV for the Co and Cu L₃ absorption edges, respectively. Images were obtained with circular polarized x-rays in remanence after applying either positive or negative saturating magnetic fields. In order to obtain sufficient signal-to-noise ratios, we accumulated 400 images per magnetization direction, which were added together after aligning all images with rigid translations, in order to correct for a slight drift of the microscope during the image accumulation.

At XM-1 the samples are studied under ambient conditions, which enabled us to readily make electrical connections to each of the four lateral spin valves on every SiN membrane. For samples with small Co-contact separation we performed electrical transport measurements using lock-in techniques and a maximum electrical current of 0.5 mA. These transport measurements were performed with the sample mounted into the microscope in order to allow for simultaneous x-ray illumination and to study whether the impinging x-rays have an effect on the transport measurements.

III. RESULTS AND DISCUSSION

Non-local resistance measurements in lateral spin valves have been a powerful tool to investigate the spin injection from ferromagnetic into non-magnetic materials.^{3,11,14,15,20,21,22,23,24,25,26} A scanning electron microscope (SEM) image of a typical Co/Cu lateral spin valve with 200-nm separation between ferromagnetic contacts is shown in Fig. 1. The same figure shows the schematic non-local transport measurement geometry, where a spin polarized electrical current is injected from the Co into the Cu and drained towards one end of the Cu wire, while the resultant spin accumulation in the vicinity of the injection contact is measured with a second Co contact, towards the opposite end, outside of the direct path of the electrical current. Measuring the voltage as a function of the relative magnetization orientation of the two ferromagnetic contacts gives rise to a voltage contrast that is directly proportional to the spin accumulation.³ This is shown in Fig. 2(a), where the non-local resistance (the voltage normalized by the injection current

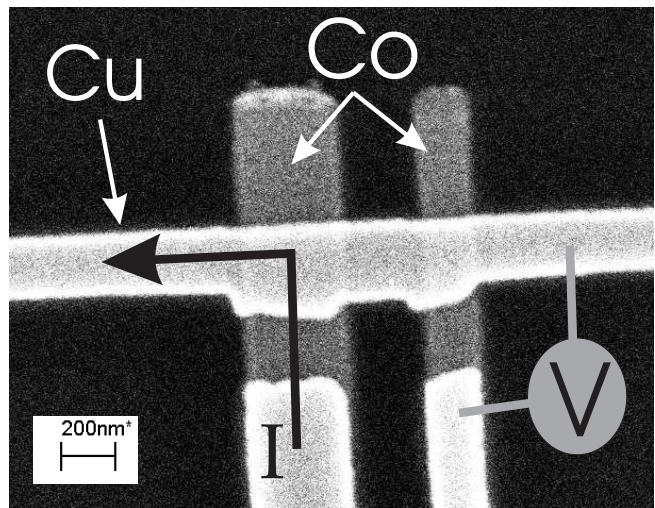


FIG. 1: SEM image of a Co/Cu spin valve with 200-nm separation between ferromagnetic electrodes. The bright parts of the device are the Cu wires, while the darker parts are the Co electrodes.

of 0.5 mA) is plotted as a function of increasing and decreasing magnetic field. The different aspect ratios of the contacts (350- and 200-nm width, respectively; as seen in Fig. 1) give rise to different switching fields and the resultant non-local resistance contrast of $\approx 30 \mu\Omega$ is consistent with earlier measurements on similar samples with a spin diffusion length of 110 nm at room temperature.^{24,27}

Apriori it is unclear whether the illumination with polarized x-rays has any influence on the spin accumulation generated by electrical injection. For example, it is conceivable that the excitation with circular polarized x-rays may either generate additional spin accumulation (similar to optical spin injection in semiconductors)^{8,28} or result in an enhanced spin relaxation. There is also the possibility that the photoelectrons generated in the x-ray absorption process disturb the balance in the spin accumulation process. To clarify this issue, we performed non-local resistance measurements while circular polarized x-rays with energies corresponding to the Co L₃ and Cu L₃ absorption edges illuminated the sample. As can be seen in Figs. 2(b) and (c) the x-ray illumination resulted in a small change of the base-signal (possibly due to generation of photoelectrons), but the non-local resistance contrast upon switching the magnetizations of the injection and detection contact remained identical to the one observed without x-ray illumination. This suggests that the impact of the impinging x-rays on the spin accumulation in the Cu wire is negligible. However, one has to realize that the electrical measurements are performed continuously with a 10-s integration period, while the x-ray illumination is pulsed with 65-ps x-ray pulse length and 2-ns pulse repetition. Since the spin relaxation time in Cu is about 1 ps,²⁷ any response to the x-ray illumination should therefore be adiabatic and the electric measurements effectively average over the illu-

minated (3.25%) and dark (96.75%) periods. Therefore, subtle changes of the electrical spin accumulation signal due to the x-ray illumination, if any, would be unresolved.

For the imaging of spin accumulation in Cu we chose a Co/Cu lateral spin valve with a 500-nm separation between injector and detector. The larger distance between the contacts will result in less structural interference of the second Co electrode with any potential spin accumulation signal. However, due to larger contact separation we were not able to directly detect the spin accumulation electrically with the sample mounted into the transmission X-ray microscope. Nevertheless, we note that earlier electrical measurements of samples with similar contact separation in a quieter environment detected the spin accumulation in Cu.²⁴ Furthermore, the electrical properties of the injector electrode (resistance) were comparable to the 200-nm separation sample discussed above. Figure 3(a) shows the TXM image taken at the Co L_3 absorption edge in remanence after both electrodes were saturated in a positive field. Both ferromagnetic Co contacts are well defined, while the contrast for the Cu wire is weak. By observing the XMCD contrast change in remanence we verified that a magnetic field of ± 840 Oe reliably switches the magnetization of both of the Co contacts. This is shown in Fig. 3(b), where images after positive and negative saturation were subtracted from each other. Note that the dark magnetic contrast is homogeneous in both electrodes, indicating that even in remanence the magnetizations remain well defined in both electrodes, which is consistent with the electrical measurements.

For investigating the spin accumulation in the Cu wire we performed MTXM imaging at the Cu L_3 absorption edge. During the image recording a spin accumulation was continuously generated via electrical injection with a *dc* 1-mA current through the wider (left in Figs. 3–5) Co electrode. Figure 4(a) shows an individual TXM image. In contrast to the images at the Co L_3 absorption edge [see Fig. 3(a)] the Cu wire and contacts are well defined by the dark contrast. In order to obtain maximum sensitivity for a potentially small XMCD contrast of the spin accumulation, we collected 400 images for each remanence with positive and negative magnetization (~ 48 hours total measurement time). In order to compensate for a slow drift of the microscope optics, all individual images were aligned using their structural contrast before being summed up [see Fig. 4(b)]. Figure 4(c) shows a line-profile of the x-ray intensity integrated across the width of the Cu wire. The positions of the Co electrodes are visible due to their additional attenuation of the x-ray intensity.

In order to obtain an image with XMCD contrast we take the difference of the individual sums of 400 images for positive and negative saturation [see Fig. 5(b)]. The XMCD contrast image does not show any distinct contrast within the area of the injection contact [see Fig. 5(a) for the corresponding structural contrast]. In order to analyze this result further we show line-profiles of the

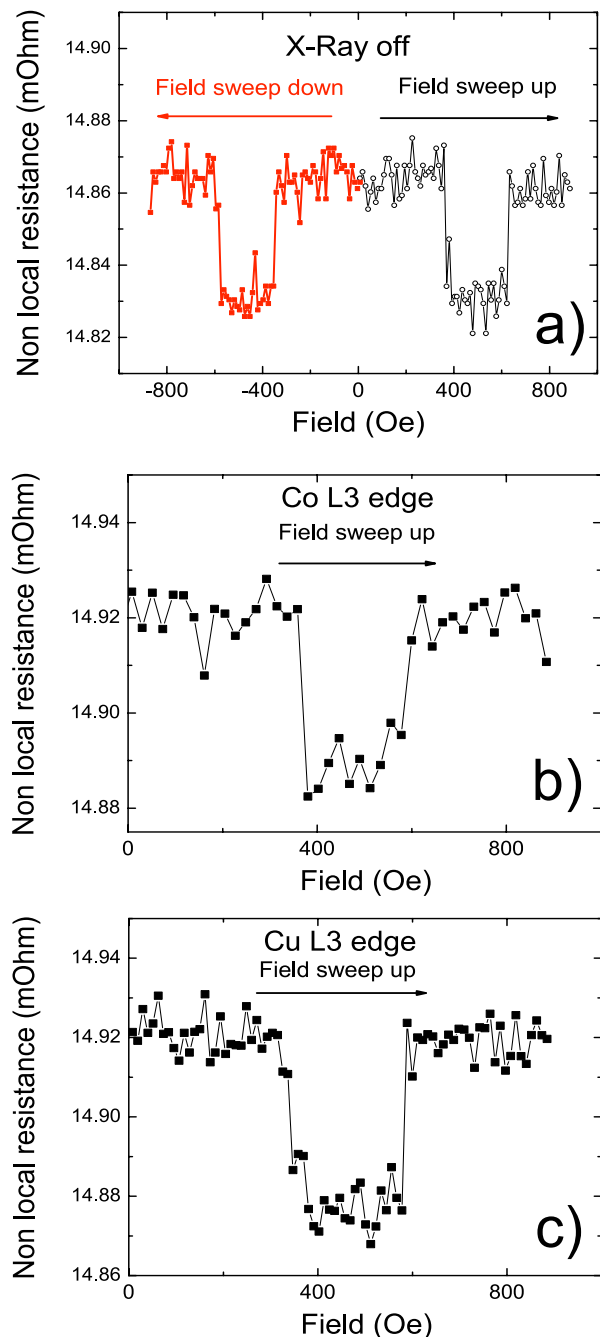


FIG. 2: (Color online) Non local electrical measurements of a Co/Cu lateral spin valve with a 200-nm separation. The change in the non-local resistance indicates a spin-accumulation in Cu and is due to the parallel *vs.* antiparallel orientation of the magnetization in the two ferromagnetic contacts. The measurements were performed (a) without x-ray illumination, and while illuminating at the (b) Co L_3 , and (c) Cu L_3 absorption edges, respectively.

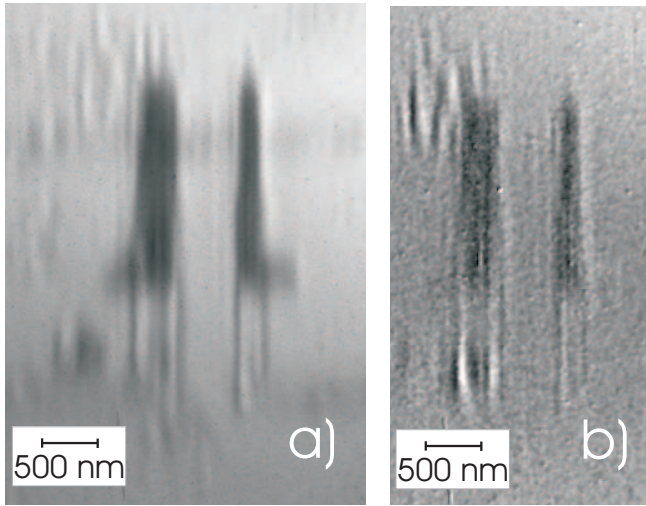


FIG. 3: (a) TXM image of a Co/Cu lateral spin valve with a 500-nm separation taken at the Co L_3 absorption edge in remanence after saturation in a positive field. The ferromagnetic Co electrodes are well defined in contrast to the barely visible Cu wires. (b) XMCD image of the same lateral Co/Cu spin valve. This image was obtained by subtracting images taken in remanence after positive and negative saturation, respectively. The dark XMCD contrast of $\sim 5\%$ indicates that the magnetization switched in both Co electrodes.

XMCD signal integrated over the width of the Cu wire [Fig. 5(c)] and in an adjacent region [Fig. 5(d)] for comparison. There is no signature of an XMCD signal from the spin accumulation in the Cu wire exceeding the noise level of data from the region without the Cu wire.

One open question is if our signal-to-noise ratio is still limited by the statistical noise. We analyzed the signal-to-noise as a function of the number N of cumulated images by calculating the ratio of the average intensity of the summed images over the noise level in the subtracted XMCD images, see Fig. 6. By taking 400 images we were able to improve sensitivity of the measurement in Cu by ~ 100 times compared to the sensitivity of a single image measurement in ferromagnetic Co. If the signal-to-noise is dominated by statistical errors, it is expected that that the signal-to-noise scales as \sqrt{N} . As can be seen in Fig. 6 the square root fit matches the data well, indicating that even after accumulating 400 images the signal-to-noise is still dominated by counting statistics. Furthermore the signal-to-noise is ~ 1700 per pixel, meaning that we are sensitive to a XMCD contrast of 0.06% /pixel. Any spin accumulation should be present over an area given by the spin diffusion length (≈ 100 nm) and thus should cover at least 15 pixels. Therefore, any XMCD contrast from a spin accumulation in Cu is $< 0.01\%$. A further reduction of the signal-to-noise is not practical. With the present experimental setup ~ 48 h of data accumulation were required with a current that is close to the limiting current density for our devices. Even with a 1 mA current the lifetime of the lateral spin valve devices is limited by elec-

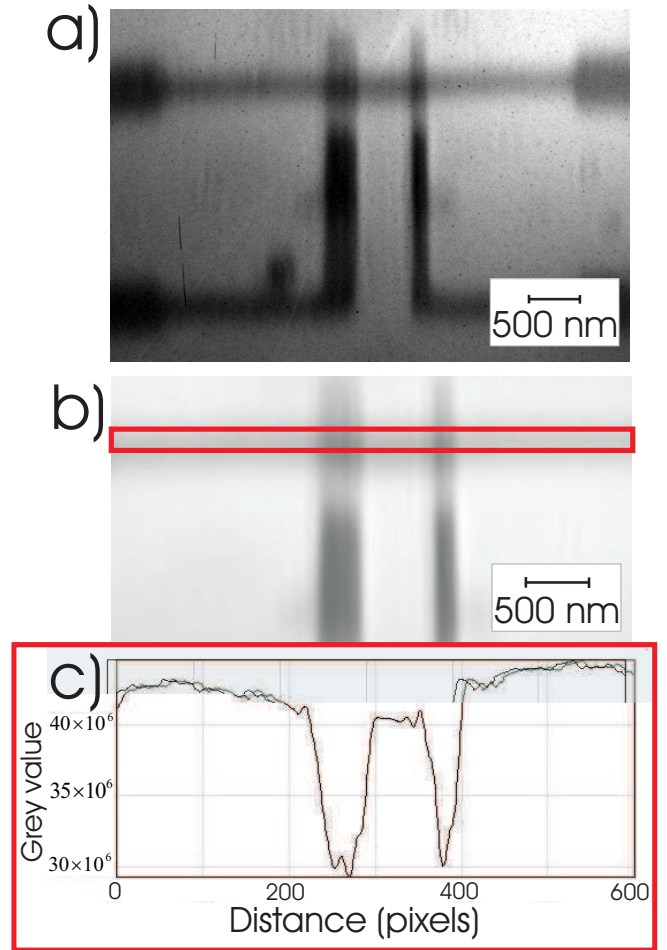


FIG. 4: (Color online) (a) Single TXM image of a Co/Cu lateral spin valve with 500-nm separation taken at the Cu L_3 absorption edge in remanence after saturation at positive field. There is a clear contrast for the Cu wires. (b) Sum of 400 images taken at the Cu L_3 absorption edge. The area of interest around the injection contact is magnified. (c) X-ray intensity profile of the summed images along the Cu wire as indicated by the rectangular box in (b). The additional attenuation of the Co electrodes is clearly visible.

tromigration and seldom exceed 2 days of a continuously applied electrical current. Thus, presently, imaging the spin accumulation with XMCD-based microscopic techniques does not seem to be a viable option.

Furthermore, the question remains whether spin accumulation should indeed result in significant XMCD contrast. The large XMCD contrast for transition metal ferromagnets stems from the large exchange splitting of the d-bands, which in turn gives rise to very different spin-dependent density of states at the Fermi level [see Fig. 7(a)] and concomitantly a different magnitude of absorption for different photon polarization states. However, the situation for spin accumulation is different, since the actual band-structure is spin-independent and the only difference is a splitting of the chemical potentials, as is schematically shown in Fig. 7(b). Unless

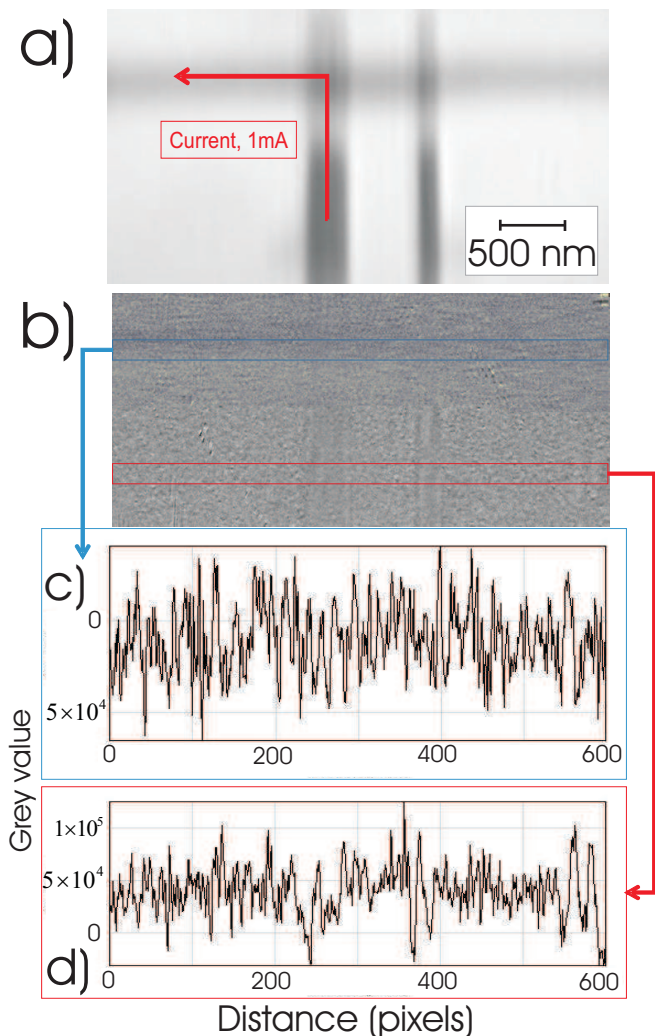


FIG. 5: (Color online) (a) Sum of 400 TXM images taken at the Cu L_3 absorption edge showing the location of the Co electrodes. The electrical current path is also indicated. (b) XMCD image of the same region obtained by subtracting summed images after positive and negative saturation. No clear magnetic contrast is observed. (c) Intensity profile of the XMCD signal integrated over the width of the Cu-wire. (d) Intensity profile of the XMCD signal integrated over the same width as in (c), but outside the region of the Cu wire. Any intensity variations in (c) are comparable to the noise in (d).

the density of states has a strong energy dependence at the Fermi energy (which would be unexpected for Cu) the absorption-rate for different photon polarizations will therefore be similar, and the only difference is a slight displacement of the absorption edge dependent on the photon polarization. From electrical measurements similar to the ones presented in Fig. 2 the measured voltage for the spin accumulation is generally at most of order of μV (see Ref.29). Thus, even taking non-perfect injection and detection efficiencies into account the splitting of the chemical potentials can be expected to be well

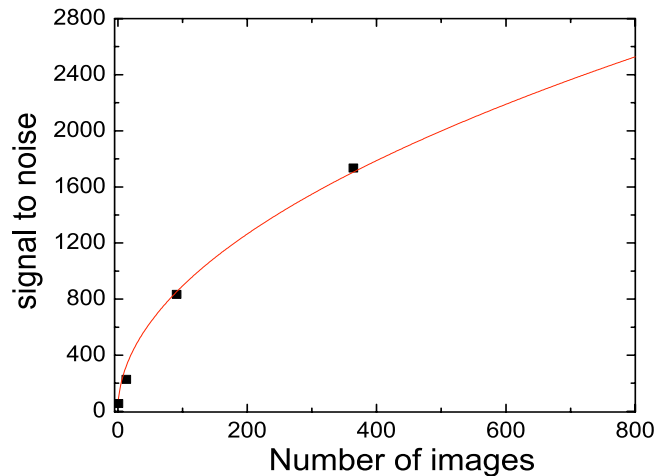


FIG. 6: Signal-to-noise ratio for each picture pixel plotted as a function of number N of summed images. \sqrt{N} fit is shown with solid line.

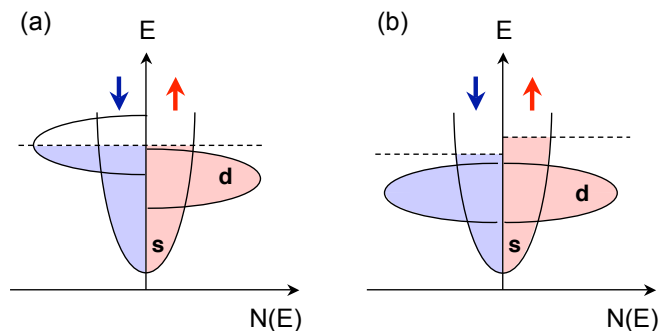


FIG. 7: (Color online) (a) Schematic band structure of a typical transition metal ferromagnet. The XMCD contrast results from the spin-dependent density of states at the Fermi level and the concomitant different absorption as a function of photon polarization. (b) Schematic band structure for spin accumulation in Cu. The spin accumulation results in a spin-dependent splitting of the chemical potential, with nearly identical density of states.

below 1 meV, and thus significantly below the energy resolution (≈ 1 eV) of our experiment. Therefore, it remains doubtful that significant XMCD contrast from a spin accumulation could be observed using the approach discussed in this paper.

IV. CONCLUSIONS

We fabricated Co/Cu lateral spin valves on free standing SiN membranes for transmission soft x-ray microscopy imaging. Non-local resistivity measurements confirmed the presence of spin accumulation in the Cu due to electrical injection from a Co electrode. The transport signature of the spin accumulation remained

unchanged under illumination with circularly polarized x-rays at both the Co and Co L₃ absorption edges. We obtained high resolution transmission x-ray microscopy images at both the Co and Cu L₃ absorption edges. However, no x-ray magnetic circular dichroism signal from the spin accumulation in Cu was observed with a signal-to-noise of 0.06% per pixel.

V. ACKNOWLEDGEMENTS

We thank V. Yefremenko and V. Novosad for their help with the SiN membrane fabrication. The CXRO and

ALS staff is highly appreciated. This work was supported by the Office of Basic Energy Sciences, Materials Sciences and Engineering Division, of the U.S. Department of Energy, under Contract Nos. DE-AC02-06CH11357 and DE-AC02-05CH11231.

-
- * Electronic address: mosendz@anl.gov
 † Electronic address: hoffmann@anl.gov
- ¹ C. Chappert and J.-V. Kim, *Nat. Phys.* **4**, 837 (2008).
 - ² A. Hoffmann, *Phys. Stat. Sol. (c)* **4**, 4236 (2007).
 - ³ M. Johnson and R. H. Silsbee, *Phys. Rev. Lett.* **55**, 1790 (1985).
 - ⁴ T. Kimura, Y. Otani, T. Sato, S. Takahashi, and S. Maekawa, *Phys. Rev. Lett.* **98**, 156601 (2007).
 - ⁵ B. Heinrich, Y. Tserkovnyak, G. Woltersdorf, A. Brataas, R. Urban, and G. Bauer, *PRL* **90**, 187601 (2003).
 - ⁶ G. Woltersdorf, O. Mosendz, B. Heinrich, and C. Back, *Phys. Rev. Lett.* **99**, 246603 (2007).
 - ⁷ O. Mosendz, G. Woltersdorf, B. Kardasz, B. Heinrich, and C. Back, *Phys. Rev. B* **79**, 224412 (2009).
 - ⁸ J. Kikkawa and D. Awschalom, *Phys. Rev. Lett.* **80**, 4313 (1998).
 - ⁹ Y. Kato, R. Myers, A. Gossard, and D. Awschalom, *Science* **306**, 1910 (2004).
 - ¹⁰ V. Sih, R. Myers, Y. Kato, W. Lau, A. Gossard, and D. Awschalom, *Nature Physics* **1**, 31 (2005).
 - ¹¹ S. A. Crooker, M. Furis, X. Lou, C. Adelman, D. L. Smith, C. J. Palmstrom, and P. A. Crowell, *Science* **309**, 2191 (2005).
 - ¹² J. Stephens, J. Berezovsky, J. P. McGuire, L. J. Sham, A. C. Gossard, and D. D. Awschalom, *Phys. Rev. Lett.* **93**, 097602 (2004).
 - ¹³ J. Bass and W. Pratt, *Journal of Physics: Condensed Matter* **19**, 183201 (2007).
 - ¹⁴ M. Urech, V. Korenivski, N. Poli, and D. B. Haviland, *Nano Lett.* **6**, 871 (2006).
 - ¹⁵ J. Hamrle, T. Kimura, Y. Otani, K. Tsukagoshi, and Y. Aoyagi, *Phys. Rev. B* **71**, 094402 (2005).
 - ¹⁶ P. Fischer, *IEEE Trans. Magn.* **44**, 1900 (2008).
 - ¹⁷ W. Chao, B. D. Harteneck, J. A. Liddle, E. H. Anderson, and D. T. Attwood, *Nature* **435**, 1213 (2005).
 - ¹⁸ P. Fischer, D.-H. Kim, W. Chao, J. A. Liddle, E. H. Anderson, and D. T. Attwood, *Mater. Today* **9**, 26 (2006).
 - ¹⁹ B. Cord, C. Dames, K. K. Berggren, and J. Aumentado, *J. Vac. Sci. Technol. B* **24**, 3139 (2006).
 - ²⁰ F. J. Jedema, A. T. Filip, and B. J. van Wees, *Nature* **410**, 345 (2001).
 - ²¹ J.-M. George, A. Fert, and G. Faini, *Phys. Rev. B* **67**, 012410 (2003).
 - ²² T. Kimura, J. Hamrle, Y. Otani, K. Tsukagoshi, and Y. Aoyagi, *Appl. Phys. Lett.* **85**, 3501 (2004).
 - ²³ Y. Ji, A. Hoffmann, J. S. Jiang, and S. D. Bader, *Appl. Phys. Lett.* **85**, 6218 (2004).
 - ²⁴ Y. Ji, A. Hoffmann, J. E. Pearson, and S. D. Bader, *Applied Physics Letters* **88**, 052509 (2006).
 - ²⁵ A. van Staa, J. Wulffhorst, A. Vogel, U. Merkt, and G. Meier, *Phys. Rev. B* **77**, 214416 (2008).
 - ²⁶ F. Casanova, A. Sharoni, M. Erekhinsky, and I. K. Schuller, *Phys. Rev. B* **79**, 184415 (2009).
 - ²⁷ Y. Ji, A. Hoffmann, J. S. Jiang, J. E. Pearson, and S. D. Bader, *J. Phys. D: Appl. Phys.* **40**, 1280 (2007).
 - ²⁸ G. Lampel, *Phys. Rev. Lett.* **20**, 491 (1968).
 - ²⁹ T. Kimura, T. Sato, and Y. Otani, *Phys. Rev. Lett.* **100**, 066602 (2008).